Fusion Engineering and Design 131 (2018) 111–118

Contents lists available at ScienceDirect

Fusion Engineering and Design

journal homepage: www.elsevier.com/locate/fusengdes

A comparative study on the performance of artificial neural networks and regression models in modeling the heat source model parameters in GTA welding

Mohammad Mahdi Tafarroj, Farhad Kolahan*

Department of Mechanical Engineering, Ferdowsi University of Mashhad, Mashhad, Iran

ARTICLE INFO

Keywords:
Heat source model
Artificial neural network
Regression
GTAW

ABSTRACT

Welding is one the most important joining methods Analytical and FEM techniques are commonly employed to model various welding processes. The heat source model is a key part of welding simulation. Proper determination of heat source parameters is one of the main factors in the accuracy of the welding simulation. In this study, artificial neural networks and regression modeling have been employed to establish the relationships between welding input variables and the parameters for the Goldak heat source model. The 27 data needed for modeling has been gathered based on full factorial design. While ANN slightly outperforms regression, both ANN and second order regression functions have good agreements with actual experiments. The approach presented here may be used to accurately specify heat source parameters for any given set of welding process variables.

1. Introduction

Various types of welding operations are well-known as the permanent joining methods. But, such techniques have some difficulties to apply including the need of skilful operators, time consuming and expensive operations. These are the reasons that the welding simulations are attended more and more. Analytical and numerical simulations are the two fields that can be replaced by welding experiments to avoid the welding difficulties. Constructing a model which describes the properties of the real welding operation accurately and precisely depends on several factors. For instance, the finite element (FE) modeling of such processes is highly affected by the simplifying assumptions, selecting the type of elements, method of heat source modeling, and etc. Among all, the heat source provides the thermal energy of welding. The temperature histories of any point of the weldment produced by the heat source have a fundamental role on the mechanical properties of the welded workpiece. One of the challenges in finite element modeling of the welded structures is to define a heat source model which is accurately able to simulate the heat input to the weldment. Usually, the parameters of a selected heat source model are estimated by using the weld bead geometry which is determined by some experiments. This procedure can undo the simplicity of the simulation. Therefore, proposing some methods to estimate the parameters of the heat source model is vital in welding simulation in terms of the hard experimental works.

Rosenthal [1] presented a moving heat source based on the Fourier theory of heat flow. But the Rosenthal model had some essential drawbacks for temperatures in or near the fusion zone (FZ) and heat affected zone (HAZ). The errors of the Rosenthal model has been discussed in detail by Myers et al. [2]. Goldak et al. [3] proposed a double ellipsoidal model for weld heat sources to simulate both the shallow and the deeper penetration arc welding processes. Furthermore, it has the possibility to apply the model for non-axisymmetric welds such as strip electrodes or dissimilar metal joining. This model has been widely applied in various studies.

A method was developed to estimate heat source parameters in welding simulation by Jia et al. [4]. They have performed a sensitivity analysis of heat source to reduce the complexity of the model. The relationships between heat source parameters and weld pool characteristics (fusion width (W), penetration depth (D) and peak temperature (Tp)) obtained with both the multiple regression analysis (MRA) and the partial least-squares regression analysis (PLSRA).

Sharma et al. [5] estimated the double ellipsoidal heat source model parameters for twin-wire application. The parameters were estimated for a different set of welding conditions.

A combined heat source model was proposed for the numerical analysis of temperature fields in keyhole PAW process by Wu et al. [6]. Belitzki et al. [7] proposed a method to simplify the finite element simulation of the welding processes. In this research, the image processing method was used to determine the weld seam contour, and the heat

* Corresponding author. Tel.: +989153114112.
E-mail address: kolahan@um.ac.ir (F. Kolahan).

https://doi.org/10.1016/j.fusengdes.2018.04.083
Received 16 August 2017; Received in revised form 9 April 2018; Accepted 20 April 2018

source parameters were calibrated using the optimization procedure. Yadaiah et al. [8] have optimized this parameter for better finite element modeling of the welding process. Then, they calculated the weld dimensions by a 3-D finite element simulation of linear GTAW process. It has been shown that the FE results were in agreement with the experiments. Using both numerical and analytical approaches, Bag et al. [9] determined the heat source model. Using the proposed method, there is no need to prior information about the final joint dimensions as a difficulty.

The brief survey of related literature showed that the heat source model is a key factor for finite element simulation of various fusion welding processes. This study aims to determine the heat source parameters based on the model first proposed by Goldak et al. [3]. For this purpose, artificial neural networks (ANN) and regression models were implemented. The main welding parameters affecting the heat source model dimensions have been considered as the input variables of the ANN and regression models. The results of both methods will be compared, and the concluding remarks will be highlighted.

2. Goldak heat source model

One of the main concerns in numerical simulation of welding is the heat source modeling. There are various methods to overcome this challenge, but most of them have some drawbacks. For example, the Rosenthal model [1] had some essential disadvantages for temperatures in or near the fusion zone (FZ) and heat affected zone (HAZ). The infinite temperature assumed in the source and the temperature dependency of the material thermal properties increases the error while the heat source is approached [10]. Pavelic et al. [11] proposed that the heat source should be distributed. They suggested a Gaussian distribution of flux which is deposited on the surface of the weldment. Although Pavelic's model is certainly an important improvement, some other authors have recommended that the heat should be distributed all over the molten zone to simulate more accurately the digging behavior of the arc. Paley [12] and Westby [13] considered a constant power density distribution in the FZ using a finite difference model, but there was no criterion to estimate the length of the molten pool in their research. Furthermore, it is not easy to accommodate the complicated geometry of the real weld pools with the finite difference approach.

As stated before, Goldak et al. [3] proposed a double ellipsoidal heat source model based on the Gaussian distribution. The proposed model was non-axisymmetric and three-dimensional. It was more realistic and more flexible model compared to the other models suggested for the weld heat sources. Using this model, both shallow and deep penetration welds can be adapted in addition to asymmetrical states. The proposed model has been shown in Fig. 1

According to this model, the power density due to the heat source is divided into two semi-ellipsoid parts: front part and rear part. The front part of the heat source is demonstrated via Eq. (1).

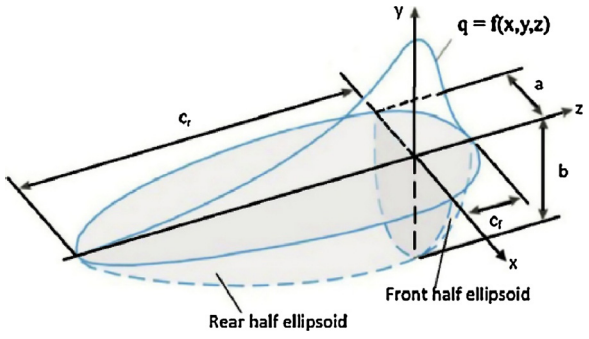

Fig. 1. Goldak's heat source model [4].

$$q_f = \frac{6\sqrt{3}f_f Q}{abc_f\pi\sqrt{\pi}} e^{-(3x^2/a^2+3y^2/b^2+3z^2/c_f^2)} \quad (1)$$

And for the rear part Eq. (2) is used.

$$q_r = \frac{6\sqrt{3}f_r Q}{abc_r\pi\sqrt{\pi}} e^{-(3x^2/a^2+3y^2/b^2+3z^2/c_r^2)} \quad (2)$$

Where, x, y, and z are the local coordinate system of the model. The parameters a and b are the semi-axes of the ellipsoids. Furthermore, c_f and c_r address the segments of axes in front and rear ellipsoids respectively. The fractions of deposited heat in front and rear of the ellipsoids are f_f and f_r respectively. These fractions are computed by Eqs. (3) and (4) [14].

$$f_f = \frac{2c_f}{c_f + c_r} \quad (3)$$

$$f_r = \frac{2c_r}{c_f + c_r} \quad (4)$$

Using Eqs. (3) and (4), it can be deduced that $f_f + f_r = 2$.
In Eqs. (1) and (2), Q is computed via Eq. (5).

$$Q = \eta IV \quad (5)$$

Where, η is the arc efficiency, I is the welding current, and V addresses the welding voltage.

In the following sections, two methods have been implemented to determine the values of heat source parameters i.e. a, b, c_f, and c_r which reduces the need for excessive experiments.

2.1. The challenges of the heat source models

One of the key parts in any heat source model is the way that the values of its parameters are specified. A main drawback in heat source modeling is that, in terms of their parameters values; they are valid only for limited ranges of welding parameters. This causes them to work accurately only under certain conditions. Traditionally, the values of heat source model parameters are determined using weld bead geometry obtained from a number of welding tests. In turn, the heat source model may be valid only for the welding parameters used in the tests performed. If the welding input parameters are significantly varied, then the parameters of the heat source model should be modified accordingly. This usually requires several welding tests using the new welding settings.

To overcome these problems, in this study, two methods have been implemented to estimate the values of Goldaks' parameters; i.e. a, b, c_f, and c_r. The advantages of the presented techniques compared to the other analytical or numerical methods are: using pure experimental data in modeling procedure, eliminating the need of considering various simplifying assumptions, eliminating the need of expensive, time consuming, and hard experiments, and reducing the computational time compared to the analytical or numerical approaches.

In this study, according to the Goldak's heat source model, four characteristics of the weld pool geometry including front and rear length of semi-ellipsoids (L_f and L_r respectively), weld width (W), and weld penetration depth (D_p) were measured. The first three aforementioned parameters were measured with 20 times magnification and the weld penetration depth was measured with 50 times magnification. The OLYMPUS SZX9 optical microscope and the image processing software, the ImageJ, were implemented as the measuring tools.

The relationships between the selected weld pool geometries and the parameters of Goldak's heat source model have been presented via the following equations:

$$a = W/2 \quad (6)$$

$$b = D_p \quad (7)$$

Table 1
Chemical compositions of the AISI 304 stainless steels.

Element	Si	C	S	Mo	Mn	Ni	Cr
Percent (%)	1	0.08	0.03	2.25	2	8–10.5	18–20

Fig. 2. PSQ 250 AC/DC (GAAM-Co, Iran) welding machine and welding torch.

Fig. 3. Automated table used in this study.

$$c_f = L_f \tag{8}$$

$$c_r = L_r \tag{9}$$

3. Experimental procedure

3.1. Materials and equipments

The gas tungsten arc welding (GTAW) process which is also known as the tungsten inert gas (TIG) welding is one of the well-known joining method. Nowadays, various researches have been conducted on the GTAW process [15,16]. In the present work, the PSQ 250 AC/DC (GAAM ELECTRIC-Co, Iran) semi-automatic welding machine with a 250 A capacity and high value of pulse frequency (up to 500 Hz) was to perform bead on plates welding of the stainless steel AISI 304. The chemical compositions of stainless steel 304 are presented in Table 1. The welding machine and the GTAW air-cooled torch with ceramic nozzle have been illustrated in Fig. 2. The 2% thoriated tungsten electrode which is the most commonly used electrodes and is preferred for their longevity and ease of use was implemented. The shielding gas was pure argon, and because the plate was thin, the welding was done without any filler metal. The plate dimensions were 100 × 40 × 1 in millimeters. Welding was started from 20 mm distance of the left side and the length of the weld line was 60 mm. Plate contaminants are cleaned before welding.

Table 2
The input parameters and the corresponding levels.

Parameter	I (A)	S (mm/min)	G (mm)
Level 1	40	230	1.6
Level 2	45	245	2.2
Level 3	55	260	2.8

Table 3
The experiment matrix and results of the heat source parameters measurements.

Experiments Number	Input			Heat source parameters			
	I (A)	S (mm/min)	G (mm)	c_f (mm)	c_r (mm)	a (mm)	b
1	40	245	2.8	0.363	0.484	0.416	0.121
2	55	260	2.8	0.759	0.932	0.772	0.31
3	40	230	1.6	0.633	0.763	0.637	0.194
4	45	230	1.6	0.674	0.853	0.1.469	0.301
5	45	245	1.6	0.575	0.872	1.432	0.218
6	40	245	2.2	0.432	0.569	1.142	0.140
7	45	260	1.6	0.466	0.619	1.290	0.204
8	55	230	1.6	0.965	1.464	1.970	0.586
9	55	260	2.2	0.823	1.057	1.738	0.402
10	45	230	2.8	0.387	0.500	1.043	0.185
11	45	230	2.2	0.600	0.705	1.374	0.263
12	55	245	1.6	0.974	1.184	1.872	0.398
13	40	230	2.8	0.380	0.465	0.848	0.132
14	40	245	1.6	0.430	0.562	1.084	0.133
15	45	245	2.8	0.488	0.607	1.237	0.184
16	45	260	2.8	0.419	0.612	1.058	0.143
17	40	260	2.8	0.312	0.435	0.879	0.130
18	45	245	2.2	0.469	0.619	1.185	0.192
19	45	260	2.2	0.495	0.614	1.148	0.199
20	40	230	2.2	0.439	0.576	0.958	0.128
21	55	245	2.8	0.842	1.163	1.773	0.439
22	40	260	1.6	0.356	0.498	1.064	0.186
23	55	245	2.2	0.876	1.094	1.660	0.349
24	40	260	2.2	0.307	0.398	0.395	0.073
25	55	230	2.2	0.927	1.204	0.989	0.473
26	55	245	1.6	0.924	0.1.185	0.897	0.414
27	55	230	2.8	0.896	1.32	0.927	0.452

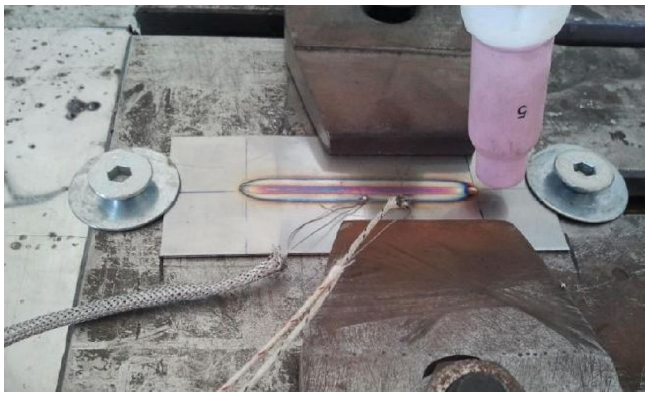

Fig. 4. A welded sample.

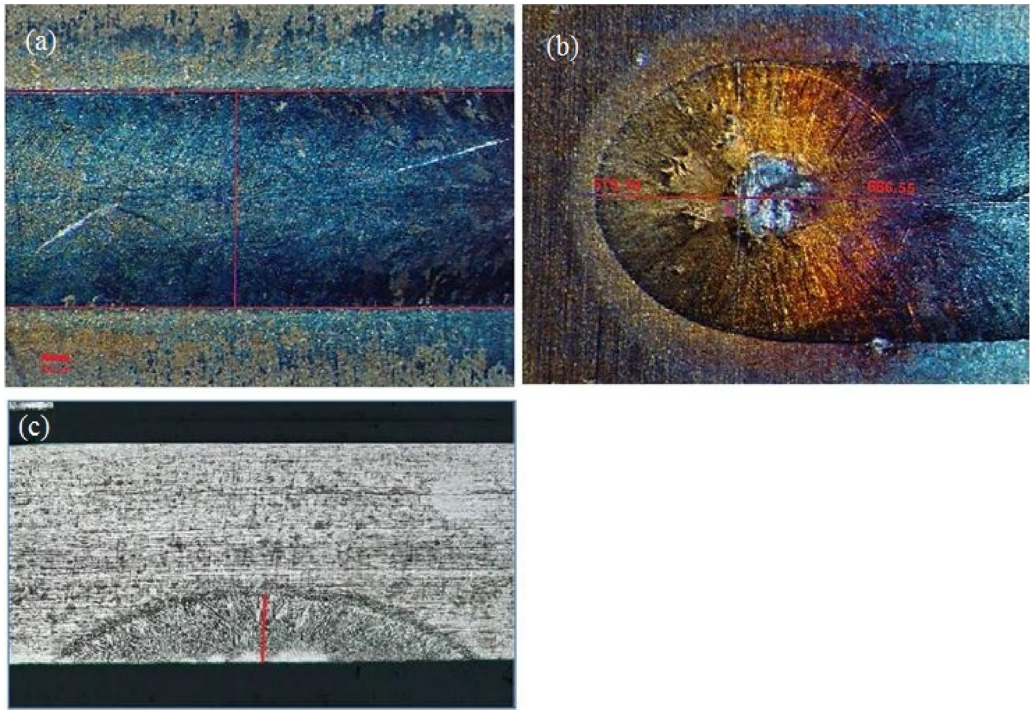

Fig. 5. Weld bead geometry measuring; (a) The weld width, (b) The front and rear length of the semi-ellipsoids, (c) Weld penetration depth.

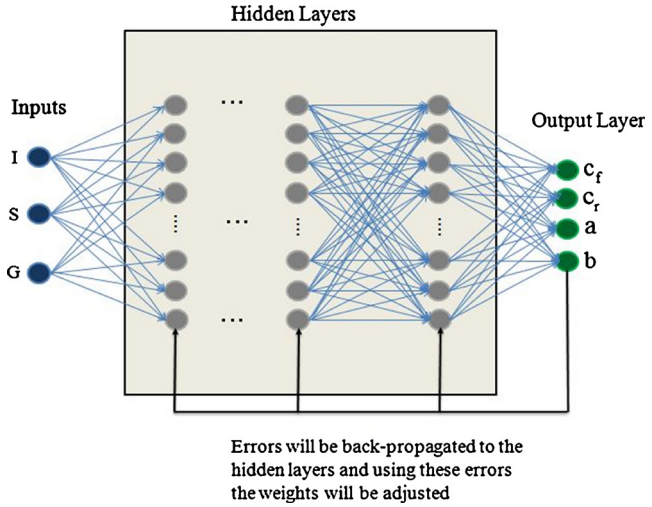

Fig. 6. The architecture of the constructed ANN.

The relative motion between the weldments and the torch was carried out using an automated table with controllable linear motion (see Fig. 3).

3.2. Design of experiments (DOE)

Effective parameters of GTAW process were selected. Various experiments also were performed to determine the upper and lower bounds of each parameter. The most effective parameters that affect the amount of heat input to the weldment are welding current (I), welding voltage (V), welding speed (S), and gap (G). The voltage is automatically tuned by the welding machine.

The parameters less important such as torch angle and gas flow rate were set to 75° and 6 L/min respectively. So, the more effective parameters in 3 levels are selected as shown in Table 2.

The full factorial design created with MINITAB software was considered according to the factors and their levels.

3.3. Performing the experiments and measuring the outputs

After setting up the required equipments and designing the experiments matrix, the specimens were welded together. The experiments matrix and the resultant outputs have been shown in Table 3.

One of the welded specimens has been shown in Fig. 4. The very simple welding fixtures and the attached thermocouples are also seen in the figure.

As an example, the images and the measured characteristics of a welded sample have been shown in Fig. 5.

4. Modeling for heat source parameters estimation

4.1. Regression model

Regression is a mathematical method which fit an approximate function to a set of *n*-tuple data. In the *n*-tuples, one element is considered as the dependent variable and the others are the independent variables. In this manner, the depended variables are approximated as a function of the independents. To know more about this methodology, one can recourse to various DOE references [17,18].

For the problem at hand, second order polynomial regression functions have been selected for process modeling. The objective is to establish the relations between the important welding input parameters (welding current, welding speed and touch to workpiece gap) and the parameters of Goldak heat source model.

4.2. Artificial neural networks (ANNs) model

The inspiration behind the artificial neural networks is the brain. The human brain consists of a huge number of processing units connected together just like a network. These units are named as “Brain Cells” or “Neurons”. An ANN is trained to find a relationship between inputs and outputs of a system. These networks are composed of some structural blocks called neurons like the biological brain cells. These blocks are very simple computational units constructing the layers in which the relation between them determines the performance of the

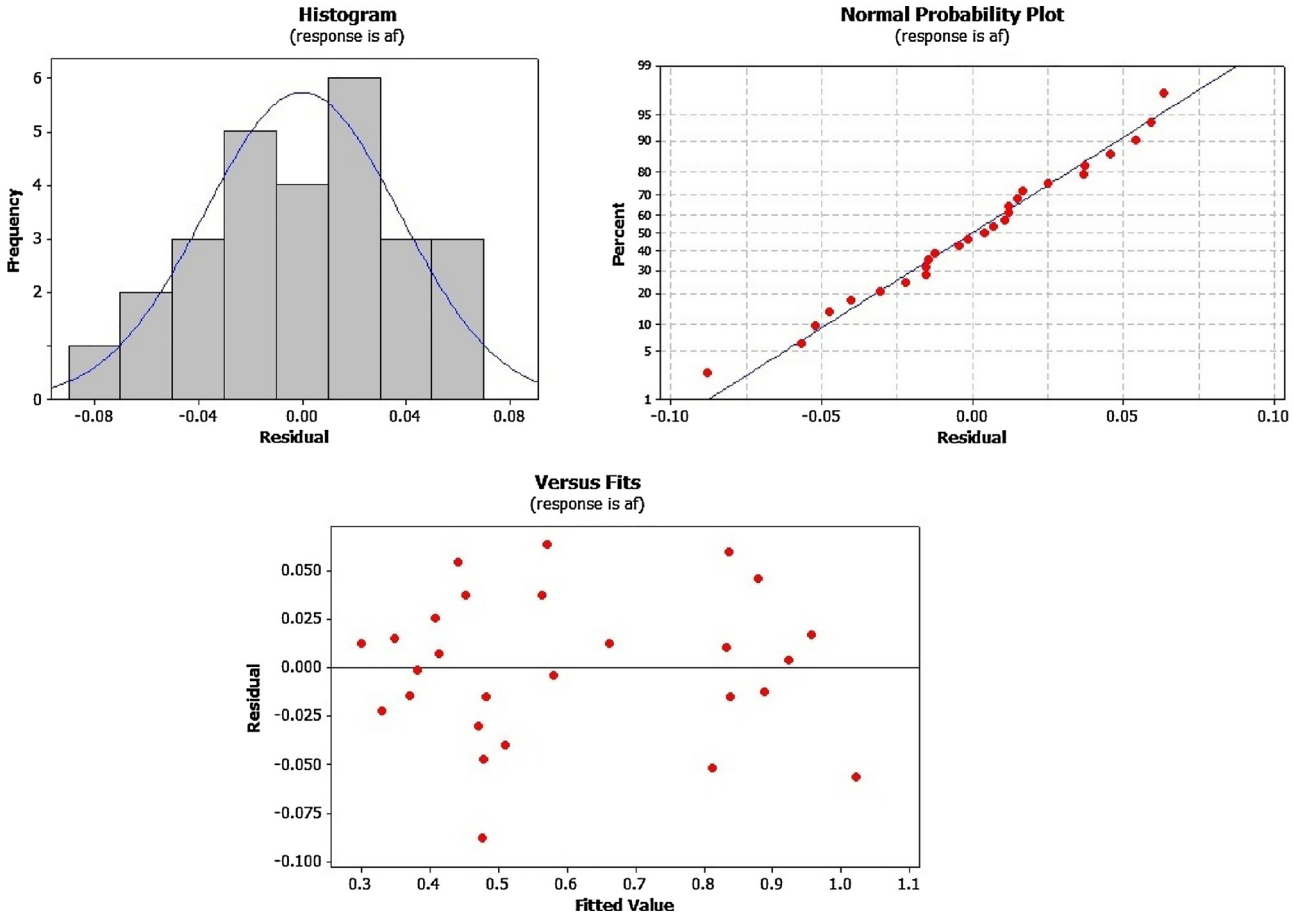

Fig. 7. Residual plots for front semi-ellipsoid data.

Table 4
The statistical characteristics of the constructed models.

Regression model	F-value	R-Sq (%)	R^2_{adj} (%)	R^2_{pred} (%)
Front semi-ellipsoid	67.1227	97.26	95.81	91.46
Rear semi-ellipsoid	44.0510	95.89	93.71	87.54
Weld width	46.6737	96.11	94.05	90.61
Weld penetration depth	37.4883	95.20	92.66	87.40

Table 5
Input parameters for validation tests.

Experiment Number	Parameter		
	I (A)	S (mm/min)	G (mm)
1	50	252	2.5
2	50	240	2

network. Neurons are arranged in such a structure that the output of every neuron in each layer is weighted and then acts as the input of the next layer. A simple representation of ANN architecture with three inputs, one output, and two hidden layers has been shown in Fig. 6. The number of hidden layers, inputs, outputs, and neurons in each layer can be variable depending on the problem.

In this work, a feedforward backpropagation neural network has been implemented to model the relationships between the welding variables and the heat source parameters. More details about this type of networks have been presented in references [19,20].

The number of hidden layers and their corresponding neurons is determined after some trials and errors [21]. Therefore, in this research, a network with one hidden layer (containing three neurons), three inputs, and four outputs has been considered. Levenberg–Marquardt algorithm was used as the training method. Tangent sigmoid and linear functions computed via Eqs. (10) and (11) were respectively selected as the activation functions in neurons of hidden layers and outputs.

The data listed in Table 3 were divided into three sets such as 0.70, 0.15, and 0.15 of all data are randomly selected as the training, testing, and validating sets respectively. To construct the neural network, the software MATLAB 2014b was implemented.

$$f(x) = x \tag{10}$$

$$f(x) = \frac{2}{1 + e^{-2x}} - 1 \tag{11}$$

5. Results and discussion

5.1. Results of the regression modeling

As stated before, second order polynomial regression model was selected to determine the heat source parameters using MINITAB software. Also, in all regression models $\alpha - level$ was assumed to be 0.05. It should be mentioned that $\alpha - level$ is called the significance level. In the subsequent analyses, the P-value is used to decide whether the regression coefficients are significantly different from zero or not. If the P-value is smaller than a pre-determined $\alpha-$level, it can be concluded that at least one of the coefficients is not zero. The constituted models for the front and rear semi-ellipsoids, the weld width, and the weld penetration depth are listed in the following. Then, the main features of four models is discussed, simultaneously.

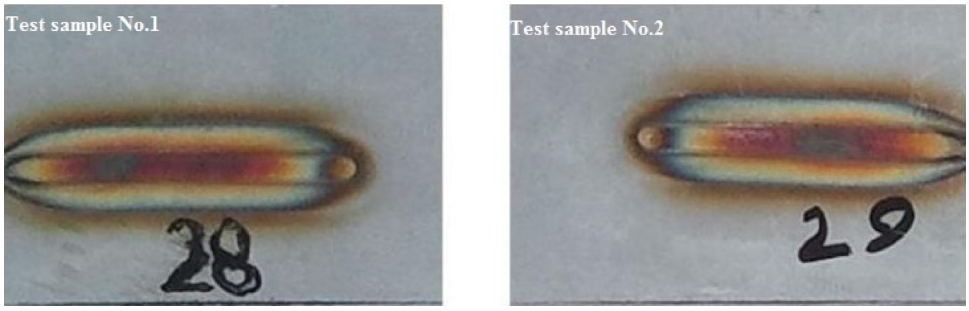

Fig. 8. The samples welded to validate the models.

Table 6
Validation of the regression models.

Heat source parameters		c_f (mm)	c_r (mm)	a (mm)	b (mm)
Outputs of regression model	Test #1	0.608	0.785	0.703	0.260
Test results		0.619	0.786	0.712	0.251
Relative error (%)		1.78	0.13	1.26	3.59
Outputs of regression model	Test #2	0.726	0.869	0.792	0.343
Test results		0.700	0.942	0.802	0.322
Relative error (%)		3.71	7.75	1.25	6.25

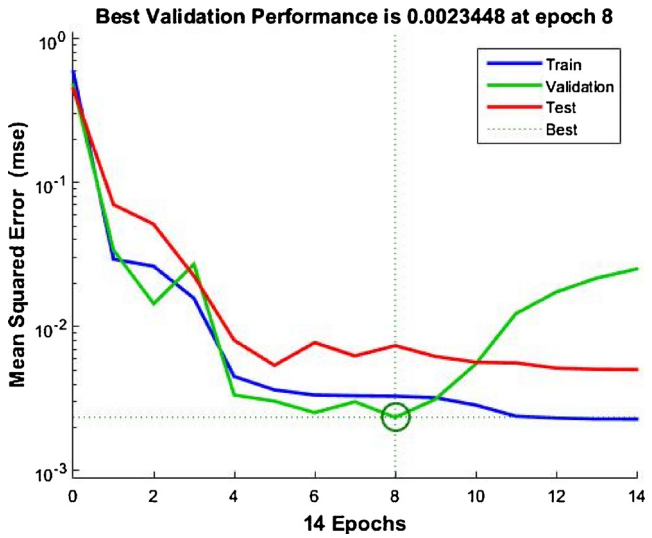

Fig. 9. Mean square error during the network training.

- Front semi-ellipsoid modeling

The modified second order regression model for the Goldak's front semi-ellipsoid is presented by Eq. (12).

$$c_f = 4.12013 - 0.110389I + 0.000469444S - 1.0214G + 0.0011637I^2 + 0.000185476IS + 0.00186508IG - 7.55556e-005S^2 + 0.00490278SG + 0.0165123G^2 \quad (12)$$

Fig. 7 illustrates the residual plots of the model. According to the figure, the residuals are normal and the data are normally distributed. It has been also seen that the randomness of data has been guaranteed.

To keep away prolixity, hereafter, the tables of ANOVA and the residual plots are not presented.

- Rear semi-ellipsoid modeling

$$c_r = 1.66356 - 0.027427I + 0.0194778S - 1.88G + 0.0015556I^2 - 0.000467857IS + 0.00115476IG - 6e-005S^2 + 0.00655556SG + 0.130556G^2 \quad (13)$$

- Weld width modeling

$$2a = -5.71533 + 0.096864I + 0.0721667S - 1.53207G + 0.000157778I^2 - 0.000440952IS + 0.0078373IG - 0.000202778S^2 + 0.0041944SG + 0.0570988G^2 \quad (14)$$

- Weld penetration depth modeling

$$b = 5.77905 + 0.0362159I - 0.0708194S - 0.41591G + 0.000466667I^2 - 0.000348095IS - 0.00100794IG + 0.000237222S^2 + 0.00126389SG + 0.0450617G^2 \quad (15)$$

The statistical characteristics of the models are presented in Table 4. Regarding to the F-distribution tables, it can be seen that for the selected $\alpha - level$, the F-values are greater than the critical values of F. Therefore, it can be argued that all models are well suited. Moreover, the high values of R-Sq, R^2_{adj}, and R^2_{pred} prove that in all cases the models are fitted to the data very well. Specially, the values of the R^2_{pred} clarify that the models can predict the outputs of new input data precisely.

In order to verify the performance of the models, two samples were welded with new input data (see Table 5). Then, the corresponding weld pool geometries are measured and their heat source parameters are obtained using Eqs. (12)–(15). Fig. 8 shows the two welded samples for testing the models constructed in this study. The results of models validation has been presented in Table 6.

It can be seen that for the test number 1, the maximum value of the relative error is 3.59% and the average of all error values is only 1.69%. For the test number 2, these values are 7.75% and 4.74%, respectively.

5.2. Results of the artificial neural networks (ANNs) modeling

Fig. 9 represents the mean square error (MSE) during the training procedure of the network. The green line shows the validation error during the training process. It should be explained that the validation is a part of the training procedure. When the data sets are divided into two subsets (train data and test data), during the training procedure, the network training error may continuously decrease. But, when the test data are presented to the trained network, sometimes it has been found that the test errors are high. In these cases, the network has been over-trained. To avoid such a problem, the third data set is used known as the validation set. In each iteration after the network is trained; theses data (known as the validation data) is applied to evaluate the error (called the validation error). When the error falls below a certain

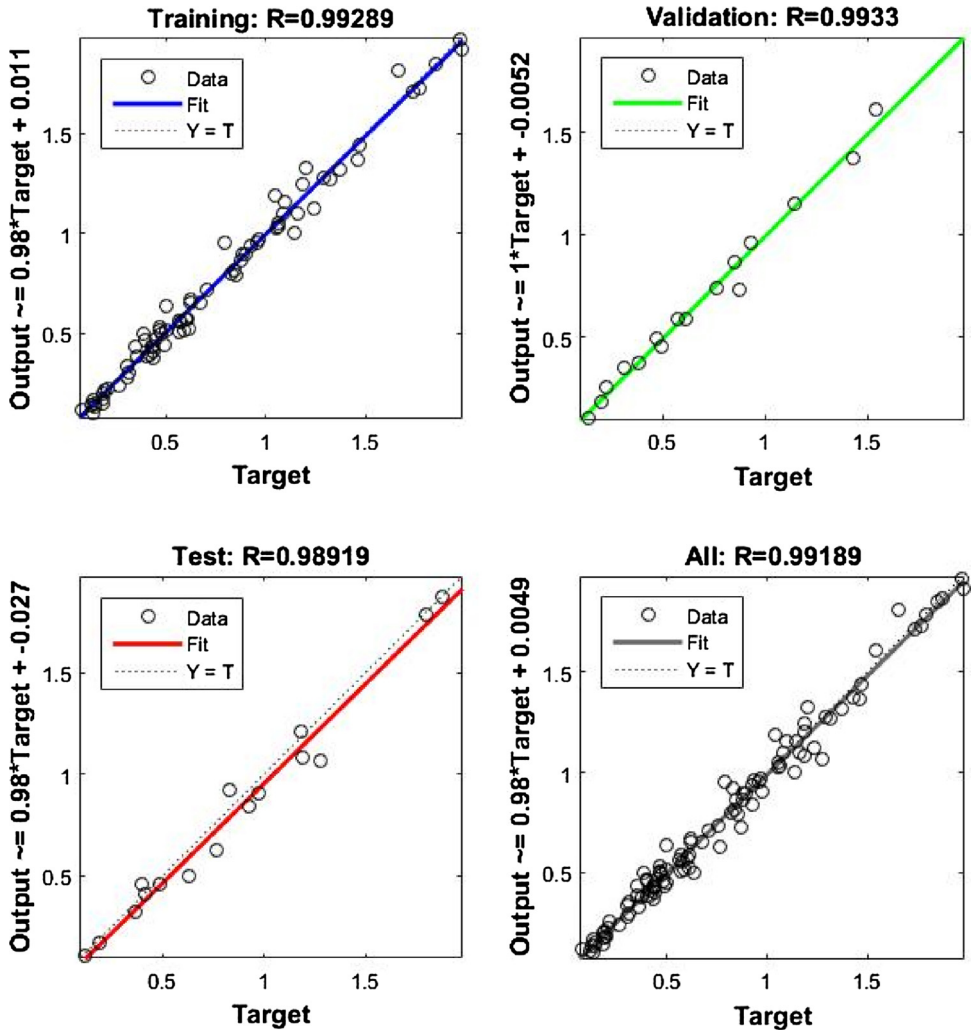

Fig. 10. Regression plots of data sets.

Table 7
Validation of the constructed ANN.

Heat source parameters		c_f (mm)	c_r (mm)	a (mm)	b (mm)
Outputs of ANN model	Test #1	0.608	0.785	0.703	0.260
Test results		0.611	0.746	0.708	0.268
Error (%)		0.49	2.67	0.71	3.07
Outputs of ANN model	Test #2	0.726	0.869	0.792	0.343
Test results		0.727	0.895	0.802	0.332
Error (%)		0.13	2.99	1.26	3.20

value, the network training stops. According to the figure, it is observed that the best answers have been found after 8 epochs. In this point, the least validation error is 0.0023448.

Fig. 10 shows the regression plots of the data sets. Figs. 9 and 10 prove that the network has been well trained and it can be used for future outputs prediction of the process.

The performance of the designed network was also evaluated via the inputs of the test samples which were presented in Table 5. The results of the network and validation tests have been shown in Table 7.

According to the results revealed in Table 7, the maximum number of relative errors is 3.07% and 3.20% for the test numbers 1 and 2, respectively. Furthermore, the average of all errors is 1.74% and 1.90% for the test numbers 1 and 2, respectively.

As another way to show the accuracy of the models, a 2D schematic view of the heat source which is generated using the parameters

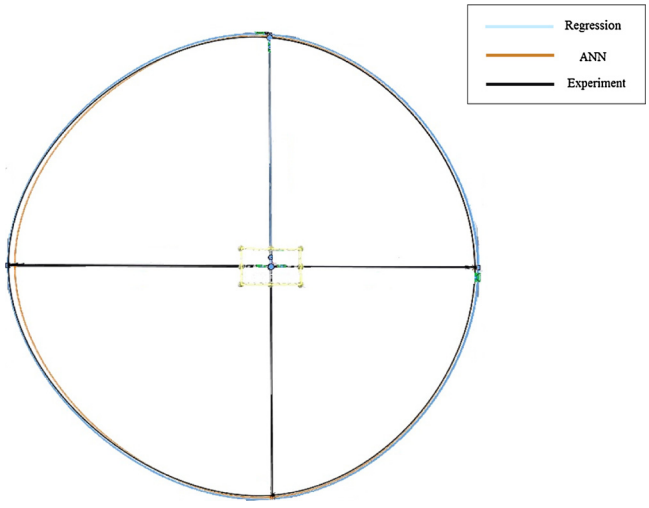

Fig. 11. Heat source generated according to test number 1.

obtained by the two models as well as the validation experiments has been illustrated in Figs. 11 and 12.

With regards to Tables 6 and 7, one can simply conclude that both ANN and regression models are capable to predict the Goldak's heat source parameters very well. In general, the ANN model has lower error

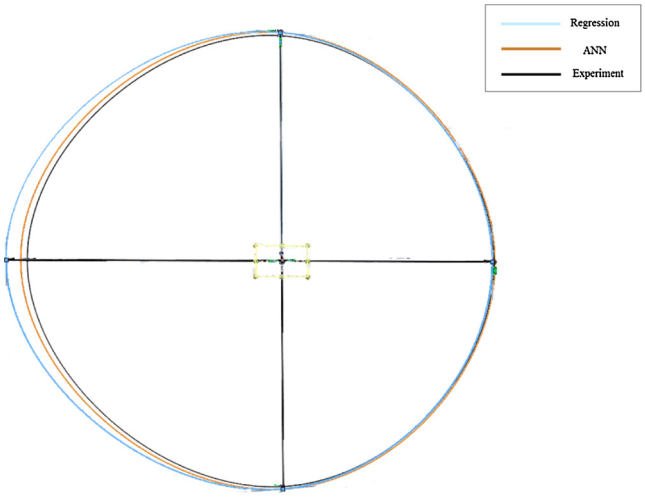

Fig. 12. Heat source generated according to test number 2.

values. But, on the other hand, the construction and execution of regression models is easier than the neural networks. If the regression model is constructed well, it is recommended to use this method due to the simplicity. Otherwise, the ANN is highly recommended. Both models can be used for further analyses and using them may surmount or reduce the need of experimental procedures especially in thermal analysis validations of welding finite element modeling.

6. Conclusion

This study introduces modeling and estimating the Goldak's heat source parameters using ANN and regression models. The results revealed that both model have excellent sufficiency to estimate the heat source parameters. In regression model, the average relative errors computed for all Goldak parameters are 1.69% and 4.74% for test samples. On the other hand, the average relative errors computed via the results obtained from the ANN are 1.74% and 1.90%. Thus, it can be said that the ANN is generally more precise, but the differences are not such that the regression models are completely ignored. Despite of its lower accuracy and precision compared to the ANN, regression method has the advantage of simple construction and implementation. Using the presented methodologies, the Goldak parameters can be acquired and then these estimated parameters can be employed to simulate the welding process via FEM. Although traditional approaches for determining the Goldak parameters need to perform new experiments when the welding conditions change, in such a way recommended here, the engineer would not be worry about the changing of welding conditions. The other superiority of these models is that the destructive methods demands for measuring the weld pool geometry are completely eliminated or at least reduced considerably.

References

[1] D.R.-T. of ASME, undefined 1946, The Theory of Moving Sources of Heat and Its Application of Metal Treatments, Ci.nii.ac.jp. (n.d.). https://ci.nii.ac.jp/naid/10004812806/. (Accessed 19 March 2018).
[2] P.S. Myers, O.A. Uyehara, G.L. Borman, Fundamentals of heat flow in welding, Weld. Res. Counc. Bull. (1967) 1.
[3] J. Goldak, A. Chakravarti, M. Bibby, A new finite element model for welding heat sources, Metall. Trans. B 15 (1984) 299–305, http://dx.doi.org/10.1007/BF02667333.
[4] X. Jia, J. Xu, Z. Liu, S. Huang, Y. Fan, Z.S.-F.E. Design, undefined 2014, A new method to estimate heat source parameters in gas metal arc welding simulation process, Elsevier. (n.d.). https://www.sciencedirect.com/science/article/pii/S0920379613007047. (Accessed 19 March 2018).
[5] A. Sharma, A.K. Chaudhary, N. Arora, B.K. Mishra, Estimation of heat source model parameters for twin-wire submerged arc welding, Int. J. Adv. Manuf. Technol. 45 (2009) 1096–1103, http://dx.doi.org/10.1007/s00170-009-2046-3.
[6] C. Wu, Q. Hu, J.G.-C.M. Science, undefined 2009, An adaptive heat source model for finite-element analysis of keyhole plasma arc welding, Elsevier. (n.d.). https://www.sciencedirect.com/science/article/pii/S0927025609000779. (Accessed 19 March 2018).
[7] A. Belitzki, C. Marder, A. Huissel, M.F. Zaeh, Automated heat source calibration for the numerical simulation of laser beam welded components, Prod. Eng. 10 (2016) 129–136, http://dx.doi.org/10.1007/s11740-016-0664-9.
[8] N. Yadaiah, S.B.-I. international, undefined 2012, Effect of heat source parameters in thermal and mechanical analysis of linear GTA welding process, Jstage.jst.go.jp. (n.d.). https://www.jstage.jst.go.jp/article/isijinternational/52/11/52_2069/_article/-char/ja/. (Accessed 19 March 2018).
[9] S. Bag, D.V. Kiran, A.A. Syed, A. De, Efficient estimation of volumetric heat source in fusion welding process simulation, Weld. World 56 (2012) 88–97, http://dx.doi.org/10.1007/BF03321399.
[10] J.A. Goldak, M. Akhlaghi, Computational Welding Mechanics, (2005), http://dx.doi.org/10.1007/b101137.
[11] V. Pavelic, R. Tanbakuchi, O.A. Uyehara, P.S. Myers, Experimental and computed temperature histories in gas tungsten-arc welding of thin plates, WELD J. 48 (1969) 295.
[12] Z. Paley, P.H.-W. journal, undefined 1975, Computation of temperatures in actual weld designs, Files.aws.org. (n.d.). http://files.aws.org/wj/supplement/WJ_1975_11_s385.pdf. (Accessed 19 March 2018).
[13] O. Westby, Temperature Distribution in the Work Piece by Welding, (1968) https://scholar.google.com/scholar?hl=en&as_sdt=0%2C5&q=Temperature+Distribution+in+the+Work+Piece+by+Welding&btnG= . (Accessed 19 March 2018).
[14] J. Park, G. An, H.L.-M. Design, undefined 2012, Effect of external load on angular distortion in fillet welding, Elsevier. (n.d.). https://www.sciencedirect.com/science/article/pii/S0261306912003792. (Accessed 19 March 2018).
[15] X. Li, J. Chen, P. Hua, K. Chen, W. Kong, H. Chu, Y. Wu, W. Zhou, Effect of post weld heat treatment on the microstructure and properties of Laser-TIG hybrid welded joints for CLAM steel, Fusion Eng. Des. 128 (2018) 175–181, http://dx.doi.org/10.1016/J.FUSENGDES.2018.02.034.
[16] S. Liu, J. Sun, F. Wei, M. Lu, Numerical simulation and experimental research on temperature and stress fields in TIG welding for plate of RAFM steel, Fusion Eng. Des. (2018), http://dx.doi.org/10.1016/j.fusengdes.2018.03.058.
[17] J. Kleijnen, Design and Analysis of Simulation Experiments, (2008) https://link.springer.com/content/pdf/10.1007/978-3-319-18087-8.pdf . (Accessed 19 March 2018).
[18] D.C. Montgomery, Design and Analysis of Experiments, John wiley & sons, 2007.
[19] D. Graupe, Principles of Artificial Neural Networks, (2013) https://books.google.com/books?hl=en&lr=&id=W6W6CgAAQBAJ&oi=fnd&pg=PR7&dq=Principles+of+artificial+neural+networks&ots=X1p3cHoPPj&sig=V_X87FrciZogKYsD4YqyDCUmurw . (Accessed 19 March 2018).
[20] M. Hagan, H. Demuth, M. Beale, Neural Network Design, (1996) https://pdfs.semanticscholar.org/2cfa/de1b02be1d21d94a0f63ca620f66c838097e.pdf . (Accessed 19 March 2018).
[21] G.E. Cook, R.J. Barnett, K. Andersen, A.M. Strauss, Weld modeling and control using artificial neural networks, IEEE Trans. Ind. Appl. 31 (1995) 1484–1491.